Dynamic Indentation of Lightweight Sandwich Panels

D.W. Zhou, W.J. Stronge

Department of Engineering, University of Cambridge, Trumpington Street, Cambridge CB2 1PZ, UK

Abstract

Slow speed impact by a small mass can cause residual indentation without perforation of a fibrous core sandwich panel. Here, we develop a dynamic axisymmetric structural model of panel indentation by assuming that there is elastic bending of the faceplate with membrane stretching while the fibrous core is plastically deformed. Finite element analysis using ABAQUS was performed to validate the analytical model. Collision experiments were carried out on HSSA fibrous core sandwich panels that were struck at different velocities; these measurements were compared with both the theoretical analysis and the numerical simulation.

1. INTRODUCTION

Ultra-light sandwich panels are increasingly desirable and interesting for scientists and engineers because of their high bending stiffness per unit area density. Generally, the faceplates of sandwich panels consist of metals or laminated composites while the core is made of corrugated sheet, foam, or honeycomb. One drawback of sandwich panels is that they exhibit relatively low resistance to localized impact damage of the surface, i.e. denting; this occurs because the core is weak in normal compression. The present research is investigating the dynamic indentation of thin, lightweight sandwich panels.

Originally, many analytical methods for calculating panel indentation have involved the Hertz contact law to describe the local deformation. However, this is inappropriate since the indentation of a panel is dominated by the local deformation of the core [1]. In general, the indentation depends on the faceplates, core, indenter shape, and boundary conditions. Currently, most research on dynamic indentation of sandwich panels is focused on those with a core composed of honeycomb or foam with composite faceplates [2-8]. However, since the mechanical properties of the core depend on the microstructure or physical arrangement and connectivity, the properties of each type of core must be analyzed independently.

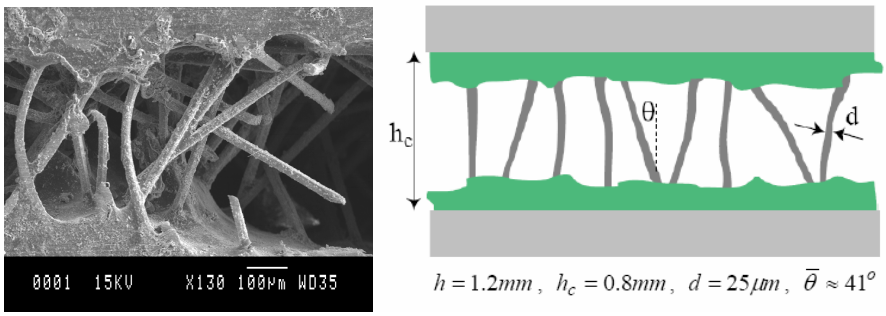

Fig. 1. SEM micrograph and schematic depiction of the fibrous sandwich structure (HSSA)

Metallic panels with a special fibrous core have recently been developed. An example of this new thin and lightweight sandwich panel can be seen in Fig. 1. This sandwich material, called HSSA, consists of stainless steel plates (316L) that sandwich a core composed of stainless fibres which are aligned roughly perpendicular to the faceplates. The total thickness of this panel is only 1.2 mm – a thickness which is distinctive from that of other common panels where the thickness $h \geq 10\,\text{mm}$.

This paper addresses the static and dynamic indentation behavior of sandwich panels with fibrous core. The core is assumed to be rigid-perfectly plastic because the yield stress of the fibrous core is quite small. In particular, attention is paid to HSSA fibrous sandwich panel impacted at a relatively slow speed by a small mass.

2. MATERIAL

As seen in Fig. 1, the fibrous core has a non-periodical distribution of fibres. In addition, most of the fibres have an initial curvature; these details greatly affect the mechanical properties of the core, making the core have a low stiffness and strength in the through-thickness direction. Measurement has shown that HSSA has a through-thickness Young's modulus of about 100 MPa [9]. Other basic parameters of this material are given in Table 1. A static through-thickness compression test of the core is shown in Fig. 2.

Table 1. Mechanical properties of HSSA fibrous core

	Faceplate	Fibrous Core*	Single Fibre
Density (Kg /m^3)	7800	624	7800
Poisson Ratio	0.3	0	0.3
Young's modulus (MPa)	210,000	100	210,000
Yield Stress (MPa)	306	1.9 – 2.3	1,100

* Through – thickness direction

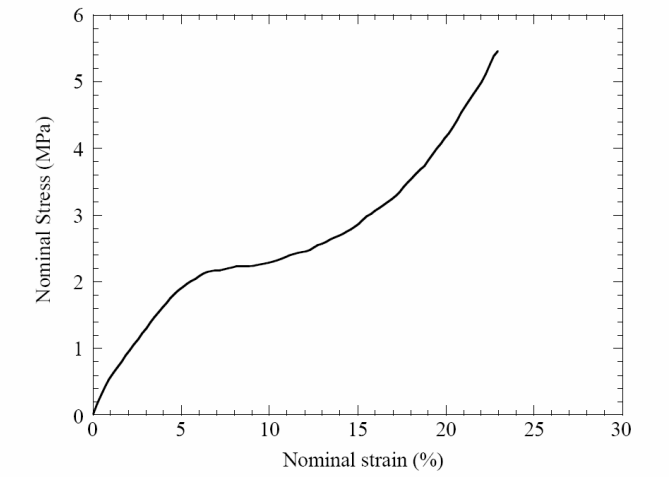

Fig. 2. Through-thickness compression test on HSSA fibrous core sandwich panel [10]

From Fig. 2, it can be seen that fibrous core has a very low yield stress which is around 2.0 MPa at a strain of 4%. The curve then enters a plateau stage in which the stress increases gradually to 3 Mpa at a strain of 16%. Thereafter, the core begins to densify and the stress increases sharply. Because the local impact damage of these sandwich panels is mainly dependent on the core behaviour, the fibrous core sandwich panel is not as resistant to denting as the corresponding monolithic steel plate in terms of dynamic indentation. Experiments below will validate this tendency.

3. EXPERIMENT

A drop test was carried out to determine the experimental damage on HSSA panel caused by the normal impact of a steel sphere. The experiment consists of a spherical steel ball, which has a diameter of 14.28 mm and a mass of 11.88 g, impacting onto an HSSA panel (either 135 mm x 40 mm or 150 mm x 50 mm) at a range of speeds from 1 m/s to 2.5 m/s. In order to compare the energy absorption ability with that of a traditional monolithic steel plate, the corresponding test on a plate with the same faceplate material (316L) and a thickness of 0.4 mm was also preformed (this thickness is identical to the combined thickness of faceplates of HSSA panel). Both the HSSA panels and the monolithic steel plate rested on a rigid foundation, which results in only local deformation. In the test, the ball dropped freely from a series of heights (from 10 cm-30 cm at intervals of 5 cm). The profile of the residual indentation was measured by a “Surfcom” profile meter, which can give accuracy of the residual indentation depth on the order of a micrometer. At least three independent tests for each impact height were performed and measured to reduce the error. The indentation depth was obtained from the average value.

4. ANALYTICAL MODEL

Some typical assumptions for low speed impact problems are used here. In general, the velocity of impact is low compared to the velocity of the wave propagation in the sandwich panel. The load-force relation can be obtained by studying the quasi-static problem. The impactor is treated as rigid body. The mass of the impactor is much greater than that of the faceplate; hence the mass of the faceplate can be ignored when studying the impact response of the panel. For the particular example of a fibrous core sandwich panel, as illustrated in Fig. 2 and Fig. 4, it can be assumed that the core is rigid-perfectly plastic since the yield stress is small and the maximum indentation depth of the panel is less than 20% of the core thickness. During the process of indentation, the faceplate bends elastically and may have large deflection compared with the thickness of the faceplate. The membrane stress therefore should be considered and corresponding thin plate large deflection theory, rather than the Kirchhoff plate theory, will be used. In the following derivation, an approximate formula for the contact law based on the principle of minimum potential energy will be given.

As shown in Fig. 3, the shape of the deflected surface can be represented by the same equations as in the case of small deflections under uniformly loaded clamped circular plates

$$w = \delta(1 - \frac{r^2}{a^2})^2 \tag{1}$$

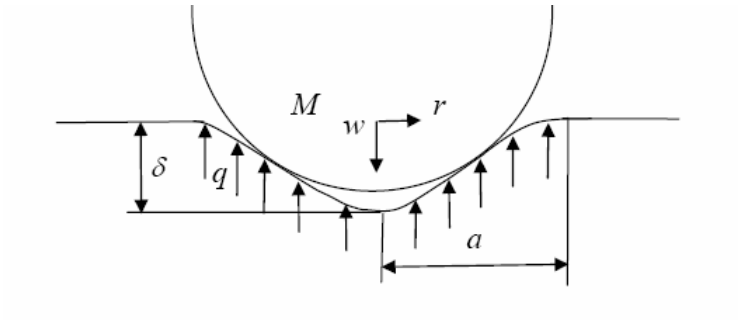

Fig. 3. Schematic of a spherical ball impacting onto the sandwich panel

where δ is the maximum deflection amplitude and a is the contact size. The corresponding bending energy is given by [11]

$$V_1 = \frac{D}{2}\int_0^{2\pi}\int_0^a \left[\left(\frac{\partial^2 w}{\partial r^2}\right)^2 + \frac{1}{r^2}\left(\frac{\partial w}{\partial r}\right)^2 + \frac{2\nu}{r}\frac{\partial w}{\partial r}\frac{\partial^2 w}{\partial r^2}\right] r dr d\theta \tag{2}$$

where $D = Eh_f{}^3\left[12(1-\nu^2)\right]^{-1}$ is the bending stiffness of the faceplate in which E, h_f, and ν are the Young's modulus, thickness and Poisson ratio of the faceplate, respectively. The radial displacements can be approximately expressed as

$$u = r(a-r)(A+Br) \tag{3}$$

and the corresponding strain energy due to membrane stretching is

$$V_2 = 2\pi\int_0^a\left(\frac{N_r\varepsilon_r}{2} + \frac{N_t\varepsilon_t}{2}\right) r dr = \frac{\pi E h_f}{(1-\nu^2)}\int_0^a (\varepsilon_r{}^2 + \varepsilon_t{}^2 + 2\nu\varepsilon_r\varepsilon_t) r dr \tag{4}$$

where ε_r and ε_t are the axial and tangential strain respectively. Taking the derivatives of the stretching energy with respect to *A* and *B* respectively and equating them to zero, we obtain the coefficients *A* and *B,*

$$A = \frac{\delta^2(179-89\nu)}{126a^3} \qquad B = \frac{\delta^2(13\nu-79)}{42a^4} \tag{5}$$

The plastic work done by the core is written as

$$D = 2\pi \int_0^a qwrdr \tag{6}$$

The work done by the external force P is given by

$$U = -P\delta \tag{7}$$

The total potential energy can be therefore written as

$$\prod = V_1 + V_2 + D + U \tag{8}$$

Substituting Eqs. (2) - (7) into Eq. (8) and minimizing the total potential energy with respect to the deflection amplitude δ, i.e., $\frac{\partial \prod}{\partial \delta} = 0$, yields

$$P = \frac{64\pi D\delta}{3a^2}\left[1 + \frac{\delta^2\left(7505 + 4250\nu - 2791\nu^2\right)}{17640{h_f}^2}\right] + \frac{\pi q a^2}{3} \tag{9}$$

Minimizing the load P with respect to the damage size a and combining Eq. (9) gives

$$P = \frac{16\pi}{3}\sqrt{Dq\delta(1 + \frac{\left(7505 + 4250\nu - 2791\nu^2\right)\delta^2}{17640{h_f}^2})} \tag{10}$$

Eq. (10) gives the contact law of sandwich panel with membrane stretching which indicates that the contact force is not proportional to the deflection – a result that occurs in the case of an elastic core [1]. This is also in contrast with the well known Hertz law which says

$$P \propto \delta^{3/2} \tag{11}$$

Specifically, the above relationship for the Poisson ratio of 0.3 becomes

$$P = \frac{16\pi}{3}\sqrt{Dq\delta(1 + 0.488\frac{\delta^2}{{h_f}^2})} \tag{12}$$

The impact response of the rigidly supported sandwich panel can be calculated

$$M\ddot{\delta}(t) = -P \tag{13}$$

or

$$\frac{dT}{d\delta} = -P \tag{14}$$

where the kinetic energy $T = M\dot{\delta}^2/2$ and M is the projectile mass. The maximum indentation, maximum contact force and during of impact can be resolved numerically according to Eqs. (13) or (14). For the maximum contact time, however, we find that the integral results can be approximated as

$$t_{\max} \approx \frac{1.7\delta}{V_0} \tag{15}$$

5. FEM SIMULATION

The commercial finite element code, ABAQUS 6.3, has been used to simulate the impact for comparison with the results of the experimental drop test and analytical modelling. The mesh arrangement of the model is shown in Fig. 4. The colliding body is assumed to be rigid with the same parameters as specified in the experimental study. No friction between the sphere and the plate is considered because the impact is normal to the faceplate. The FEM model of the panel has a radius that is roughly 5 times the maximum radius of the contact area. This is reasonable since the loads are quite localized and further analysis shows that the stresses in the core and faceplates sharply die out within a small distance from the contact zone. All parts of the sandwich panel are meshed with 4-node axisymmetric, bilinear elements with two degrees of freedom at each node, namely, CAX4R elements with reduced integration. Both faceplates have four elements through the thickness while the core has 16 elements near the impact zone and 8 elements far away from the impact area. Convergence studies indicate that this mesh is fine enough to accurately simulate the core. Perfect bonding is assumed to occur between core and faceplates. The bottom faceplate has displacements constrained in both *x*- and *z*- directions and symmetry boundary conditions are prescribed on the axis of symmetry.

The faceplate is assumed to behave as an elastic-plastic material with strain hardening behaviour. For the fibrous core, it is hard to find an accurate model in existing plasticity theories because it is transversely isotropic in the elastic part and pressure dependent in the plastic area. At the moment, both crushable foam and the Drucker-Prager material models have been investigated for simulation of the core. Detailed theoretical explanation of the crushable foam model can be found in paper [12]. In the case of the extended Drucker-Prager model [13], biaxial experimental results suggest that the failure envelope observes the Mohr-Coulomb criterion although there is wide scatter in the data [14-15]. Thus, the parameters of the extended Drucker-Prager model can be directly calculated from the Mohr-Coulomb parameters. The frictional angle in the experiment ranges from 16^o – 52^o. In the present model, an average value of 34^o is used as the representative angle. Note this value is larger than the threshold of 22^o for matching Mohr-Coulomb and Drucker-Prager models with low frictional angles. ABAQUS suggests that the ratio of yield stress in triaxial tension to yield stress in triaxial compression, *K*, should be taken as 0.778 in this circumstance (the extended model becomes the original Drucker-Prager model when *K=1*) [13]. One drawback of both plasticity models in ABAQUS is that only linear isotropic elasticity is available. Isotropic hardening of the core is considered by using the uniaxial compression yield stress–strain curve. Although both models

allow either associated or non–associated flow law, the associated flow law is used for simplification. Further investigation of non–associated flow law shows that the difference between results is not large.

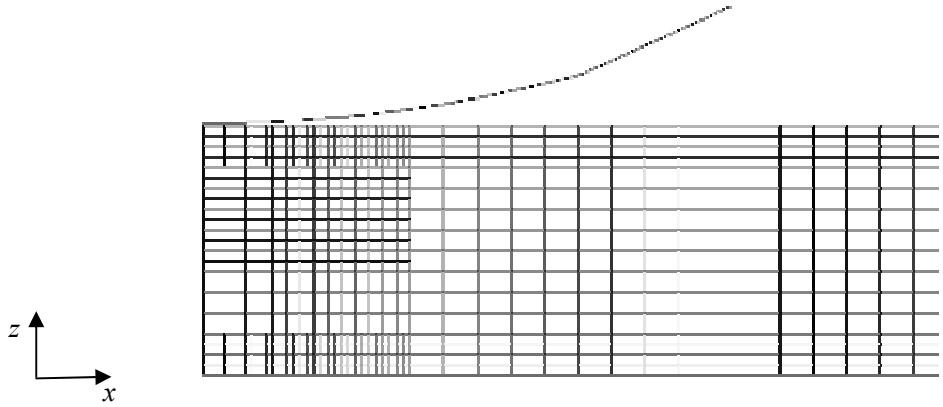

Fig. 4. Mesh of HSSA sandwich panel for dynamic analysis

6 RESULTS & DISCUSSIONS

Fig. 5 shows the relation between the residual indentation depth and impact energy for HSSA panels and monolithic steel plates. It can be seen that the residual indentation depth of HSSA panels is significantly greater than that of monolithic steel plates when hit at the same impact energy. Thus, because of the thin faceplate used in fabricating HSSA panels, this material is given plastic indentation more easily than monolithic sheet material. A comparison of the crushable foam model with Drucker-Prager model is also given in Fig. 5. It is straightforward to see that the Drucker-Prager model is much more accurate than the crushable foam model for the residual indentation depth, although there is still a noticeable difference when the impact energy is small. In the following numerical simulation, the FEM model refers solely to the model based on Drucker-Prager plasticity theory unless stated otherwise. Further observation of Fig. 5 shows that the residual indentation of HSSA panel asymptotically approximates a limit value as the impact energy increases. This indicates that the influence of the core hardening behavior is becoming dominant.

A comparison of the indentation profile obtained from the FEM simulation with the experiment can be seen in Fig. 6. It can be seen that the surface profile of the FEM model qualitatively agrees with that of the experiment. The effect of piling up around the indentation (i.e., upward displacement) can be also found in both experimental and FEM results. It is known that this is readily to occur for strain-hardened material. Hence, this phenomenon suggests that the fibrous core sandwich material performs more like a strain-hardened material, rather than strain-hardening.

Fig. 7 (a) gives a comparison of the indentation obtained from the analytical model with FEM simulations as functions of time. It can be seen that the results of these two models are identical in the loading phase before the maximum indentation arrives. Fig. 7 (b) gives the corresponding curve of monolithic stainless steel sheet that has the same thickness as the two faceplates but without the core (0.4 mm). A comparison of these two figures shows that both the maximum dynamic deflection and the corresponding impact duration of monolithic steel sheet are much smaller than those of sandwich panel. There is roughly a factor of nine difference between them for the same impact energy and this occurs because the sandwich

panel has smaller stiffness. Similar differences occur in the contact force–time curve and contact force–deflection curve (see Fig. 8 and Fig. 9). In Fig. 8 (a), it can be seen there is roughly 20% difference for the maximum force between the FEM model and analytical model; this is because the analytical model ignores hardening of the core and uses an approximated deflection assumption. The FEM results also show that plastic bending of the faceplate occurs around impact region, although this is not significant.

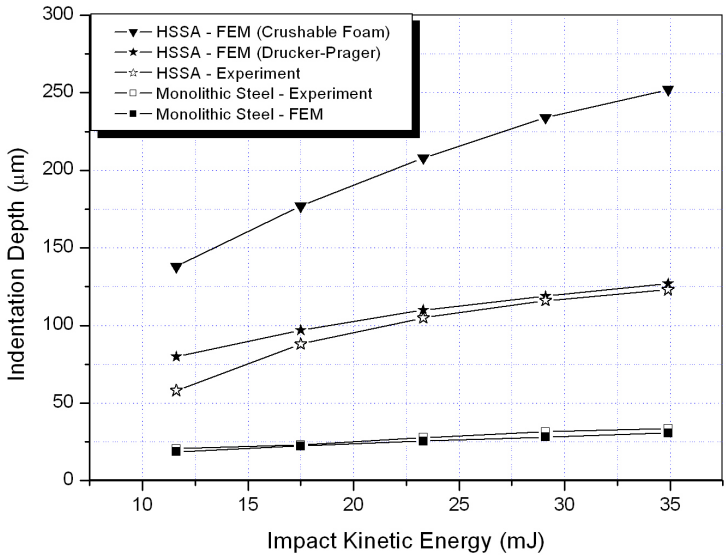

Fig. 5. Residual maximum indentation depth of HSSA in comparison with monolithic stainless steel plate (316L) from impact by a sphere

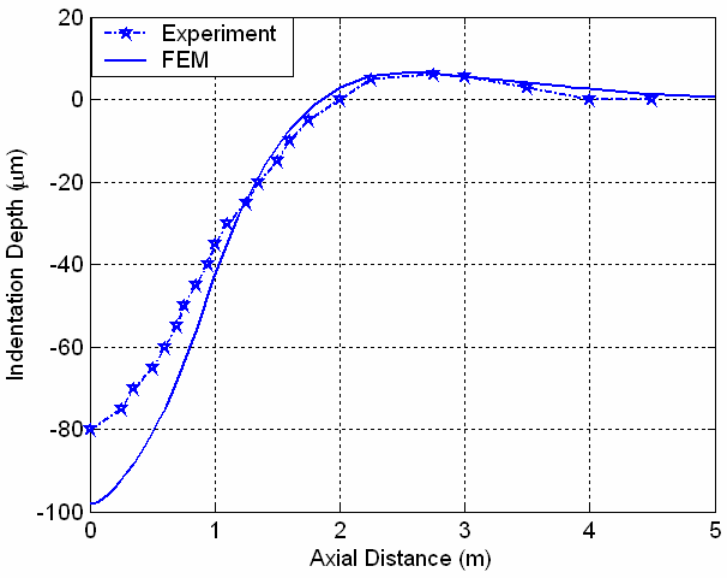

Fig.6. Comparison of residual indentation profile of the FEM model with experiment at the velocity of 1.7 m/s or impact energy 17.35 mJ

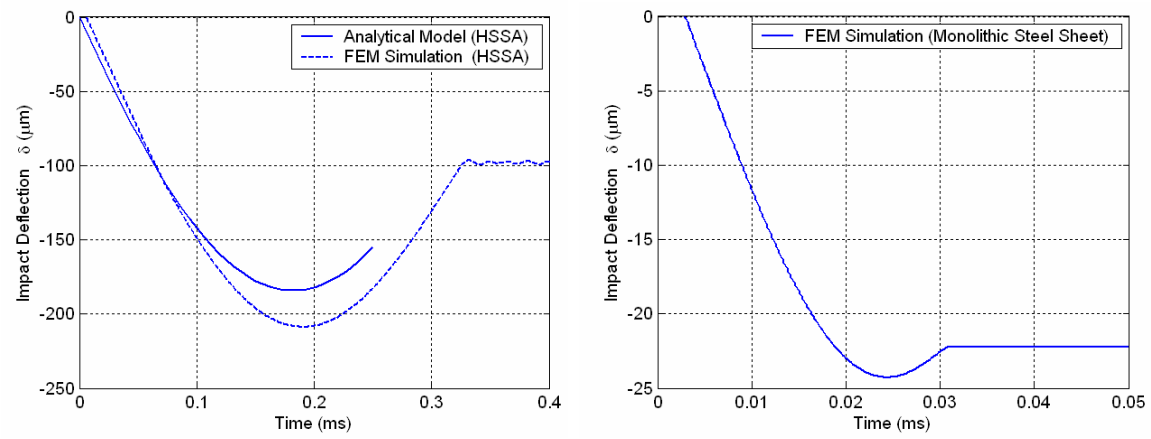

(a) (b)

Fig. 7. Dynamic indentation as a function of time at the velocity of 1.7 m/s or impact energy 17.35 mJ

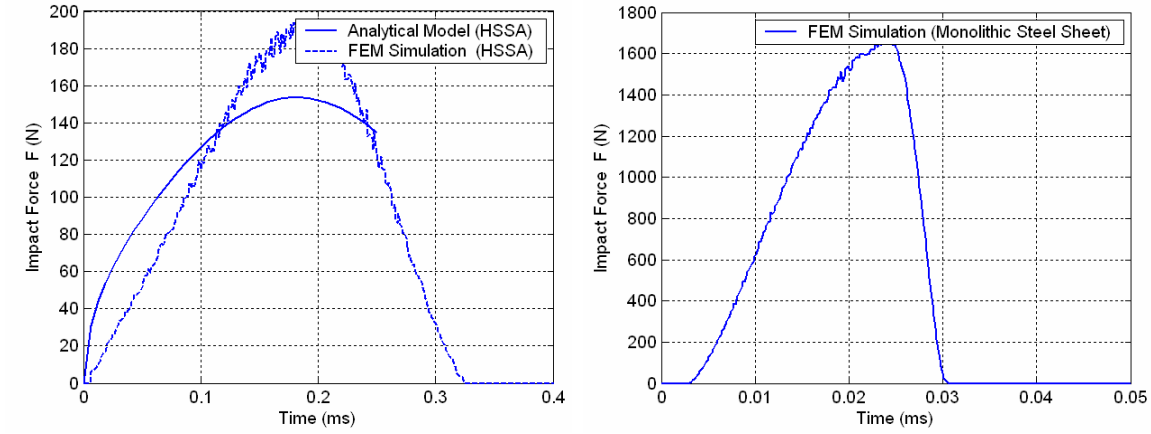

(a) (b)

Fig. 8. Contact force as a function of time at the velocity of 1.7 m/s

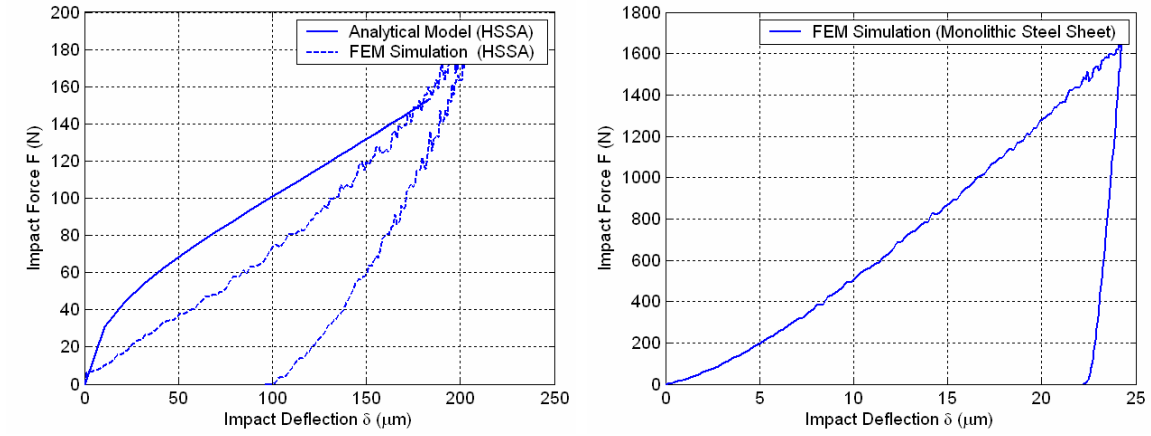

(a) (b)

Fig. 9. Contact force – deflection impact curve at the velocity of 1.7 m/s

6. CONCLUSIONS

The dynamic indentation on fibrous sandwich panel can be analytically modelled by assuming the faceplate bends elastically with membrane stretching and the core deforms as a rigid-perfectly plastic material. Numerical study shows that to represent the fibrous core in ABAQUS a Drucker-Prager plasticity model is more accurate than the crushable foam model in terms of predicting the residual indentation profile.

ACKNOWLEDGEMENTS

The authors gratefully acknowledge the financial support of Cambridge-MIT Institute (CMI). The HSSA sample was supplied by HSSA Ltd.

References

1. Abrate, S. (1997) "Localized impact on sandwich structures with laminated facings*", Appl Mech Rev.*, 50/2 (1997), 69-82.

2. Sburlati, R. "The contact behavior between a foam core sandwich plate and a rigid indentor*"*, *Composites: Part B*, 33 (2002), 325-332.

3. Lee, S.M. and Tsotsis, TK., "Indentation failure behavior of honeycomb sandwich panels", *Composites Science and Technology*, 60 (2000), 1147-1159.

4. Herup, E. J., and Palazotto, A. N. "Low-velocity impact damage initiation in graphite/epoxy/Nomex honeycomb-sandwich plates." *Composites Science and Technology,* 57/12 (1998), 1581-1598.

5. Olsson, R., and McManus, H. "Improved theory for contact indentation of sandwich panels." *AIAA Journal*, 34/6 (1996), 1238-1244.

6. Skvortsov, V., Kepler, J., and Bozhevolnaya, E. "Energy partition for ballistic penetration of sandwich panels." *International Journal of Impact Engineering*, 28/7 (2003), 697-716.

7. Soden, P. D. "Indentation of composite sandwich beams." *Journal of Strain Analysis for Engineering Design*, 31 (1996), 353-360.

8. Hoo Fatt, M. S., and Park, K. S. "Dynamic models for low-velocity impact damage of composite sandwich panels - Part A: Deformation." *Composite Structures*, 52/3-4 (2001), 335-351.

9. Markaki, A. E., and Clyne, T. W. "Mechanics of thin ultra-light stainless steel sandwich sheet metarial Part I. tiffness." *Acta Mater.*, 51 (2003), 1341-1350.

10. Markaki A. E., Clyne T. W. "Mechanical and electrical properties of stainless steel sandwich sheet with fibrous metal cores, designed for automotive applications." *Metal and Ceramic Composites: Automotive Applications, Oxford-Kobe Materials Seminar, B.Cantor(ed.)*, (2003), Submitted for publication

11. Timoshenko, S., and Woinowsky-Krieger, S. "Theory of plates and shells", McGraw-Hill, New York (1969)

12. Deshpande, V. S., and Fleck, N. A. "Isotropic constitutive models for metallic foams." *Journal of the Mechanics and Physics of Solids*, 48/6-7 (2000), 1253-1283.

13. ABAQUS/Explicit User's Manual, Version 6.3. Hibbitt, Karlsson & Sorensen, Pawtuker, RI, (2002)

14. Mohr, D. "A new method for the biaxial testing of cellular solids." *Experimental mechanics*, 43/2 (2003), 173-182.

15. Mohr, D. etc. "Biaxial Testing of the HSSA core." 3rd CMI Workshop, Cambridge, UK, (2003)